

Features of the Primate Connectome Revealed by Trade-Off Between Wiring Cost and Efficiency

Yuhan Chen * †, Shengjun Wang ‡, Claus C. Hilgetag § ¶ and Changsong Zhou □ † // □ □

*Department of Physics, Hong Kong Baptist University, Kowloon Tong, Hong Kong, China, † Centre for Nonlinear Studies, and Beijing-Hong Kong-Singapore Joint Centre for Nonlinear and Complex Systems (Hong Kong), Institute of Computational and Theoretical Studies, Hong Kong Baptist University, Kowloon Tong, Hong Kong, China, ‡ Department of Physics, Shaanxi Normal University, Xi'an, Shaanxi Province, China, § Department of Computational Neuroscience, University Medical Center Eppendorf, Hamburg, Germany, ¶ Department of Health Sciences, Boston University, Boston, MA, USA, // Beijing Computational Science Research Center, Beijing 100084, China, and □ □ Research Centre, HKBU Institute of Research and Continuing Education, Virtual University Park Building, South Area Hi-tech Industrial Park, Shenzhen, China

Email: hellen23@hkbu.edu.hk, sjwang@126.com, c.hilgetag@gmail.com, cszhou@hkbu.edu.hk

Abstract– The anatomical primate connectome has some pronounced properties, highly related to the information processing and brain disorder disease. However, the mechanism underlying the network properties, especially the relationship between the spatial layout and anatomical connectome, is not clear. This work studied the influence of two important but competing constraints of wiring cost and efficiency on the Macaque anatomical wiring diagram. It is revealed that the existence of similar modular and multiple hubs structure, even the location of hubs is attributed to a proper trade-off between the two fundamental constraints. However, the degrees of non-hubs cannot be fully explained by the two constraints. Further fixing the degrees of cortical areas, nearly 70% of connections of Macaque connectome can be recovered under the trade-off between the wiring cost and processing efficiency constraints. These findings suggest that the cost-efficiency trade-off contribute to the characteristic architecture of neural networks at different scales.

1. Introduction

The complex anatomical primate connectome is the physiological basis for brain dynamics, neural information processing and mental functions [1-3]. In recent years, the topological features of cortical connectome detected by graph theoretical approaches have attracted broad attention, such as the small world [4], densely connected modules [5], large-degree hubs [6, 7], because the pronounced features is related to information processing and brain disorders [8, 9]. However it is poorly understood about the mechanisms underlying the formation of such complex topological features, especial their relationship to the spatial layout of the anatomical connectome.

The organization of neural networks is strongly affected by fundamental constraints. The most extensively discussed constraint is the wiring cost constraint [10-13]. Most of these previous studies found that the real

component placement layout of some neural subsystems has been optimized under the wiring minimization, but not for the whole neural network [10-13]. It has been speculated that the anatomical connectome is the result of an economical trade-off between the physical cost and the functional values of the topology [14]. But it is still not clear what these functional constraints are and what the relationship is between the neural network properties and functional values

The processing efficiency, measured by processing steps across the neural network, is strongly related to minimizing noise, fast response, and even cognitive ability as well as the brain diseases [16-20]. Thus in this work, processing efficiency is taken as the representative functional value.

In the present work we explored how the anatomical Macaque connectome is shaped by the cost-efficiency trade-off by systematically testing the effect of the competition of multiple constraints. We compared the real network properties to reconstructed networks derived from multiple constraints by fixing the spatial position of each network node and the total number of connections as in the real networks. The reconstructed networks are generated by minimizing the objective function $L = (1 - \alpha) L_g + \alpha L_p$, where L_p represents the influence of the wiring cost constraint measured by the total physical distance, while L_g represents the influence of the processing efficiency constraint measured by the total graph distance of the shortest paths. At different weight values of α , the reconstructed networks were obtained by minimizing the objective function L starting from 50 random configurations by simulated annealing. Then we compared different network properties in the reconstructed networks to those in the real network. In the final part, we further fixed the degrees of all areas as in the real network, then obtained the reconstructed networks for a given α , and examined the overlap between the connections in the reconstructed networks and the real network. Our analyses provided the evidence that the

wiring cost-efficiency trade-off plays a basic role in explaining network properties.

2. Results

2.1. Cost-efficiency trade-off leads to the coexistence of hubs and local connections

For the real Macaque cortical network (Fig. 1A, B), the reconstructed networks at different α are acquired by the cost-efficiency trade-off model. At $\alpha=0$, the reconstructed networks only considered the influence of processing constraint. Thus all the links in the reconstructed network are connected randomly, which means there are a large number of long-range connections, and the wiring cost is very high (Fig. 1C). At $\alpha=1$, only the wiring cost constraint is considered. Thus all links in the reconstructed network are connected locally (Fig. 1F). There is no hub in the reconstructed network. Notably, the spatial layout of the network nodes is non-uniform in the real network (Fig. 1A), forming spatial clusters. Thus these local connections make the adjacency matrix of the reconstructed network non-uniform as shown in Fig. 1F.

When α stays between 0 and 1, the wiring cost and processing efficiency constraints combine their impact, resulting in two different regimes. When α is positive but not very large ($0 < \alpha < 0.8$), the reconstructed networks have the single global hub and all the other links connected locally. The global hub is a very effective configuration to provide high efficiency, when all the

other connections are short-distance due to the wiring cost constraint. Notably, because of the wiring cost constraint, the global hub stays in the geometrical central of the whole network area $A1$, which is not the hub in the real network. As α increases, the long-range connections of the global hub cannot meet the increasing need of the wiring cost constraint. Thus several smaller hubs emerge, staying at the local geometrical central with connections extending to nodes in their spatial neighborhood. The rest links are still connected locally. When the control parameter α is around 0.85, the local connections and multiple hubs coexist in the reconstructed network, similar to that in the real Macaque cortical network.

2.2. Similar modular structure as in the real cortical network under the cost-efficiency trade-off

We analyzed modules in the real Macaque cortical network and reconstructed networks. The modularity in the real network is $Q=0.395$, corresponding to two modules. When $\alpha=0$, the reconstructed network under the single efficiency constraint is the random network without clear modular structure ($Q=0.096$). But when α is positive, the modularity in the reconstructed network is quite large, around 0.5. Comparing the modular division between the reconstructed and real network, the number of mismatched areas achieves the minimal, only 15% of total cortical area, when α stays between 0.8 and 0.9 (shown as red stars in Fig. 2A).

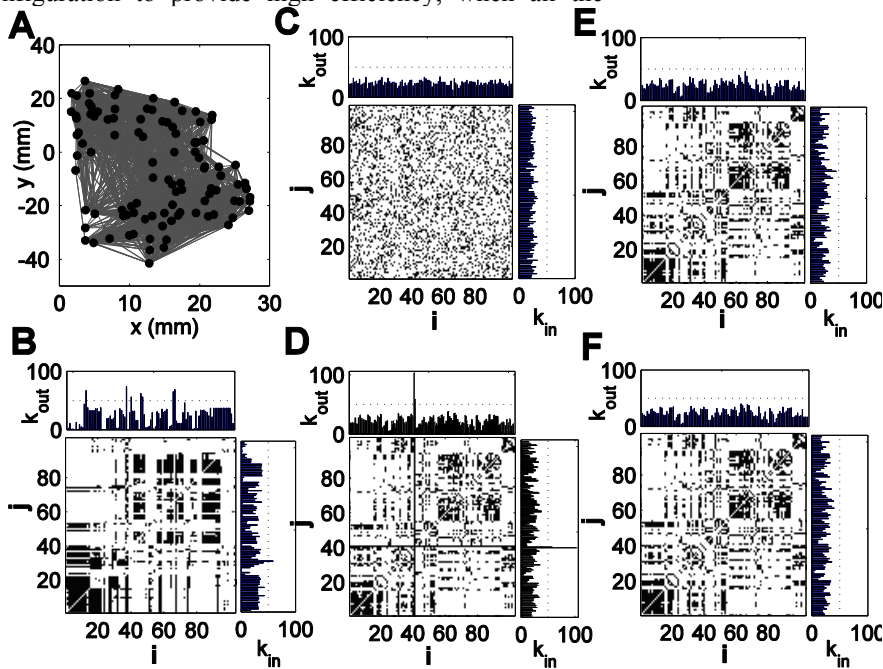


Fig. 1 Comparison of reconstructed and original connectivity of Macaque cortical network. The left two plots (A and B) are for the original network. (A) The layout placement of 103 areas and the connections between them. (B) Adjacency matrix, the output (k_{out}) and input (k_{in}) degrees of the areas. The right four plots (C-F) show adjacency matrices and the degrees of areas in the reconstructed networks at various values of α . (C) $\alpha = 0$, (D) $\alpha = 0.4$, (E) $\alpha = 0.9$ and (F) $\alpha = 1$.

2.3 Location of hubs

As stated in the first section, when α stays between 0 and 0.8, the reconstructed networks have the single global hub at the geometrical central of the whole cortical network. When $0.8 < \alpha < 0.96$, several intermediate-size hubs emerge, staying at the local geometrical central of the different modules. Especially for α around 0.9, V5/MT, area 46, MSTm and MSTd appeared as hubs (z-score above 2.0 either in total, output or input degrees). Notably, the area V5/Mt and area 46 are coincidence with the biggest hubs in the real network in terms of the total degree and out-degree respectively (two biggest green stars in Fig. 2B). They are close to geometrical centers of the two modules, shown by blue and red color in Fig. 2A. There are other 4 hubs, such as area 7a, VIP1, 7b, LIPv in the real network and they are close to the hubs in the reconstructed networks.

2.4. Degrees of cortical areas

Not only considering the hub regions, now we examine the degrees of areas in the original and reconstructed networks. Interestingly, the correlation between degrees and the number of areas within distance r is significantly present in the real network (colored curves in Fig. 2C). The correlation can reach 0.49 at $r/r_{max} \sim 0.14$ for

Macaque, much larger than the 95% of the significance level in the corresponding surrogate data (black line).

2.5 Reconstructed network under three constraints

We found that the correlation of degrees between the real and reconstructed networks is significant, but not very high, suggesting that the degrees are affected by additional unknown requirements, rather than just the cost and efficiency constraints. Thus we fixed the degrees as that in the real cortical network as the additional constraint and reconstruct networks under the cost-efficiency trade-off to explore the influence of three constraints on the anatomical Macaque cortical network.

Fig. 2D compares the recovery rate $R = \sqrt{r_0 r_1}$, where the recovery rates r_1 is for the connected pairs ($A_{ij} = 1$) while the recovery rates r_0 is for the connected pairs ($A_{ij} = 0$), as a function of α under the two constraints with that under the three constraints. R can be improved from about 60% under the two constraints up to larger than 75% under the three constraints. Notably, nearly 70% of the connections in the real network can be recovered under the three constraints (red dots in Fig. 2E). Especially, most connections (73%) within the functional systems can be recovered under the three constraints.

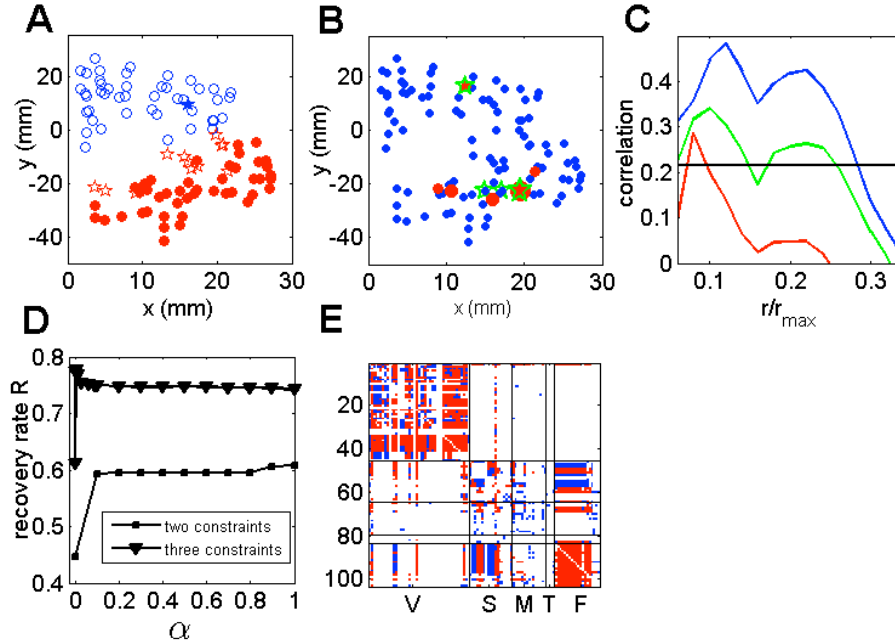


Fig. 2 Network features in the real Macaque cortical network are recovered by the reconstructed network under the cost-efficiency constraints (two constraints) or three constraints (with the degrees fixed additionally). (A) Modularity of original Macaque network and reconstructed networks. The blue and red colors represent the two modules in the reconstructed network. The mismatched areas for modular division are shown by the stars between the real and reconstructed network. (B) 6 hubs in the real network (red bullets, with the size of the symbol indicating the total degree) and 4 hubs in the reconstructed network at $\alpha \sim 0.9$ (green stars). The positions of the reconstructed or real hubs coincide or are close to each other. (C) Correlation between degrees vs. the normalized radius r/r_{max} for reconstructed ($\alpha = 0.9$) and real networks. The results differ for the output (blue line), input (red line) and total degree (green line) in the real network. (D) The recovery rates R of the two constraint schemes, without (square) and with (triangle) fixed degrees, as functions of α for Macaque. (E) The adjacent matrix of the real Macaque cortical network,

compared to the reconstructed network obtained at $\alpha = 0.006$. The red links are recovered while the blue links are not. The cortical areas are grouped by the functional systems. V: visual, S: somatosensory, M: motor, T: temporal, F: frontal system.

3. Conclusion

We studied the anatomical Macaque connectome from the perspective of multiple constraints, in particular the cost-efficiency trade-off. By reconstructing networks while preserving the spatial layout of the cortical areas, we obtained the understanding of the relationship between spatial layout and wiring diagram derived from multiple constraints. This understanding guided us to explore the mechanism of the pronounced network features in the real Macaque cortical network, namely the coexistence of modules and multiple hubs, as well as the small-world property with a large number of local connections. With the degrees further fixed, most connections within functions can be recovered under the cost-efficiency constraints. It further illustrated that the cost-efficiency trade-off have the impact on the level of the cortical-cortical connections.

4. Materials

The connectivity $\{A_{ij}\}$ of the nonhuman primate (Macaque monkey) cortical network studied in this work has $N = 103$ areas and $K = 2518$ connections in total [15]. $A_{ij} = 1$ if there is link from area j to i , and $A_{ij} = 0$ otherwise. Most of the dataset is based on the previous dataset with 94 areas [13], but improved to 103 areas with a more detailed parcellation of the motor areas based on CoCoMac [2].

Acknowledgments

This work was partially supported by Hong Kong Baptist University (HKBU) Strategic Development Fund, the Hong Kong Research Grant Council (GRF12302914), HKBU FRG2/14-15/025 and the National Natural Science Foundation of China (No. 11275027). CCH is supported by DFG grants SFB 936/A1 and HI 1286/5-1.

References

[1] K. Friston. "Beyond phrenology: what can neuroimaging tell us about distributed circuitry?" *Annual review of neuroscience*, vol. 25, 21-250, 2002.
 [2] R. Kötter, "Online retrieval, processing, and visualization of primate connectivity data from the CoCoMac database," *Neuroinformatics*, vol.2, 127-144, 2004.
 [3] N. T. Markov, et al. "Cortical high-density counterstream architectures," *Science*, vol.342, 1238406, 2013.
 [4] D. Watts, S. Strogatz. "Collective dynamics of small-world networks," *Nature*, vol.393: 440-442, 2008.
 [5] E. Bullmore, & O. Sporns, "Complex brain networks: graph theoretical analysis of structural and functional

systems," *Nature Reviews Neuroscience*, vol.10, 186-198, 2009.

[6] P. Hagmann, et al. "Mapping the structural core of human cerebral cortex," *PLoS biology*, vol.6, e159, 2008.

[7] R. L. Buckner, et al. "Cortical hubs revealed by intrinsic functional connectivity: mapping, assessment of stability, and relation to Alzheimer's disease," *The Journal of Neuroscience*, vol.29, 1860-1873, 2009.

[8] N. A. Crossley, et al. "The hubs of the human connectome are generally implicated in the anatomy of brain disorders," *Brain*, vol.137, 2382-2395, 2014.

[9] O. Sporns, "Towards network substrates of brain disorders," *Brain*, vol.137, 2117-2118, 2014.

[10] C. Cherniak, Z. Mokhtarzada, R. Rodriguez-Esteban, & K. Changizi, "Global optimization of cerebral cortex layout," *Proceedings of the National Academy of Sciences of the United States of America*, vol.101, 1081-1086, 2004.

[11] Chen, B., Hall, D., & Chklovskii, D. "Wiring optimization can relate neuronal structure and function," *Proceedings of the National Academy of Sciences of the United States of America*, vol.103, 4723-4728, 2006.

[12] Ahn, Y., Jeong, H., & Kim, B. "Wiring cost in the organization of a biological neuronal network," *Physica A: Statistical Mechanics and its Applications*, vol.367, 531-537, 2006.

[13] Kaiser, M., & Hilgetag, C. "Nonoptimal component placement, but short processing paths, due to long-distance projections in neural systems," *PLoS Computational Biology*, vol.2, e95, 2006.

[14] Bullmore, E., & Sporns, O. "The economy of brain network organization," *Nature Reviews Neuroscience*, vol.13, 336-349, 2012.

[15] Chen, Y., Wang, S. J., Hilgetag, C. C., & Zhou, C. "Trade-off between multiple constraints enables simultaneous formation of modules and hubs in neural systems," *PLOS Computational Biology*, vol.9, e1002937, 2013.

[16] Laughlin, S., & Sejnowski, T. Communication in neuronal networks. *Science*, vol.301, 1870-1874, 2003.

[17] Faisal, A., Selen, L., & Wolpert, D. "Noise in the nervous system," *Nature Reviews Neuroscience*, vol.9, 292-303, 2008.

[18] Bassett, D. S., Bullmore, E. T., Meyer-Lindenberg, A., Apud, J. A., Weinberger, D. R., & Coppola, R. "Cognitive fitness of cost-efficient brain functional networks," *Proceedings of the National Academy of Sciences*, vol.106, 11747-11752, 2009.

[20] Deary, I., Penke, L., & Johnson, W. "The neuroscience of human intelligence differences," *Nature Reviews Neuroscience*, vol.11, 201-211, 2010.